

# 超新星におけるニュートリノ反応

東理大理工 鈴木英之 @基研 2011.12.26

## 超新星ニュートリノ

$$\tau_{\text{weak}} \sim \frac{1}{\sigma_{\text{weak}} n_{\text{target}} v_{\text{relative}}} \sim 8 \cdot 10^{-8} \text{sec} \left( \frac{T}{10 \text{MeV}} \right)^{-2} \left( \frac{\rho}{10^{14} \text{g/cm}^3} \right)^{-1}$$

$$\sigma_{\text{weak}} \sim \frac{4G_F^2 \hbar^2 c^2}{\pi} T^2, n_{\text{target}} \sim \frac{\rho}{m_u}, v_{\text{relative}} \sim c$$

$$\tau_{\text{dyn}} \sim \frac{1}{\sqrt{G\rho}} \sim 0.4 \text{msec} \left( \frac{\rho}{10^{14} \text{g/cm}^3} \right)^{-1/2}$$

超新星コア中心部 ( $T \sim 10 \text{MeV}, \rho \gtrsim 10^{14} \text{g/cm}^3$ )

- コア中心部  $\tau_{\text{weak}} \ll \tau_{\text{dyn}} \Rightarrow \nu$ も熱平衡、化学平衡、 $n_\nu \sim n_\gamma \sim n_e$
- 平均自由行程  $\lambda_\nu \gg \lambda_\gamma, \lambda_e, \lambda_N$ 
  - $\Rightarrow$  ニュートリノがエネルギーを運び、コアの進化を駆動する。
  - $\Rightarrow$  ニュートリノによって超新星コアが見える。

## Energetics

$$\Delta E_G = \left( \frac{GM_{\text{core}}^2}{R_{\text{Fe core}}} - \frac{GM_{\text{core}}^2}{R_{\text{NS}}} \right) \sim O(10^{53}) \text{erg}$$

$$E_{\text{kin}} \sim O(10^{51}) \text{erg} \quad (\text{obs.})$$

$$E_{\text{rad}} \sim O(10^{49}) \text{erg} \quad (\text{obs.})$$

$$E_{GW} \sim ??$$

残り  $O(10^{53}) \text{erg} \sim E_\nu$  cf.  $E_\nu(\text{SNIa}) < 10^{49} \text{erg}$

すべての陽子が中性子に变成了としても放出される  $\nu_e$  は、

$$26 \frac{M_{\text{Fe core}}}{m_{\text{Fe}}} \langle E_{\nu_e} \rangle \sim 1.2 \cdot 10^{52} \text{erg} \frac{M_{\text{Fe core}}}{1.4 M_\odot} \frac{\langle E_{\nu_e} \rangle}{10 \text{MeV}}$$

であり  $E_{\nu \text{ tot}} \sim O(10^{53}) \text{erg}$  の 10% でしかない。

$\Rightarrow$  thermal  $\nu \gg$  電子捕獲に伴う  $\nu_e$

$\Rightarrow \nu_e, \bar{\nu}_e, \nu_\mu$  がほぼ同等に寄与

$$E_{\nu_e}(\text{collapse}) \sim 10^{51} \text{erg}$$

$$E_{\nu_e}(\text{neutronization burst}) \sim 10^{51} \text{erg}$$

$$E_\nu(\text{shocked accreted matter}) \sim 10^{53} \text{erg}$$

$$E_\nu(\text{PNScooling}) \sim 10^{53} \text{erg}$$

## 平均エネルギー

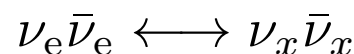
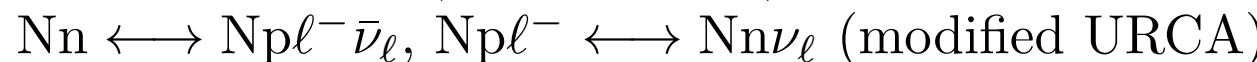
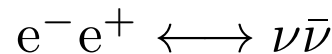
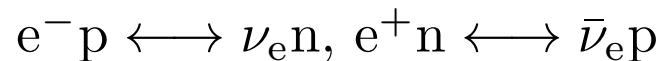
$$\begin{array}{ccccc} \sigma_{\nu_e} & > & \sigma_{\bar{\nu}_e} & > & \sigma_{\nu_\mu} \\ R(\nu_e \text{sphere}) & > & R(\bar{\nu}_e \text{sphere}) & > & R(\nu_\mu \text{sphere}) \\ T(\nu_e \text{sphere}) & < & T(\bar{\nu}_e \text{sphere}) & < & T(\nu_\mu \text{sphere}) \\ \langle \omega_{\nu_e} \rangle & < & \langle \omega_{\bar{\nu}_e} \rangle & < & \langle \omega_{\nu_\mu} \rangle \end{array}$$

## ニュートリノ反応

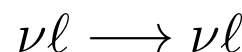
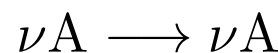
$T \lesssim 100 \text{MeV}, \rho \lesssim 10^{15} \text{g/cm}^3$ :  $\mu^\pm, \tau^\pm$  は無視することが多い

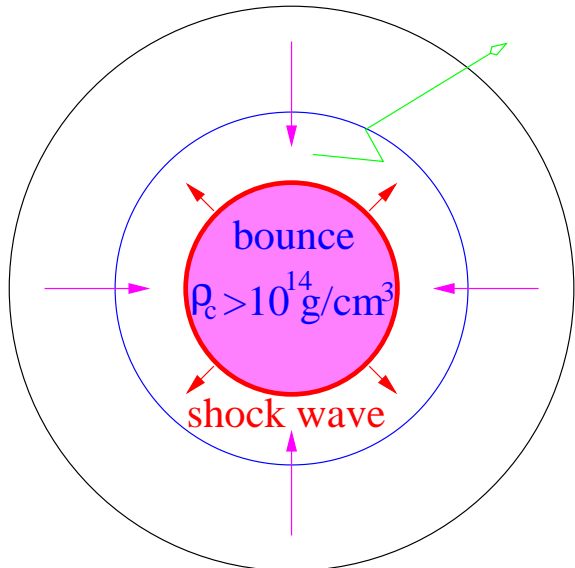
$\nu \equiv (\nu_e, \bar{\nu}_e, \nu_\mu, \bar{\nu}_\mu, \nu_\tau, \bar{\nu}_\tau)$ ,  $\nu_\mu$  または  $\nu_x = \frac{1}{4}(\nu_\mu + \bar{\nu}_\mu + \nu_\tau + \bar{\nu}_\tau)$  と記す

## 放出、吸収

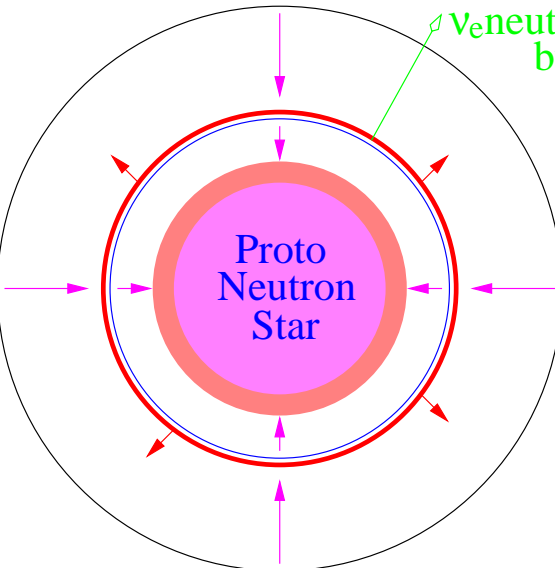


## 散乱

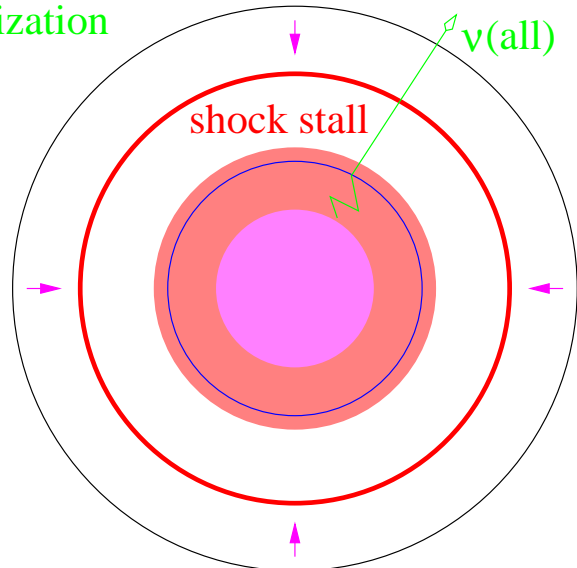




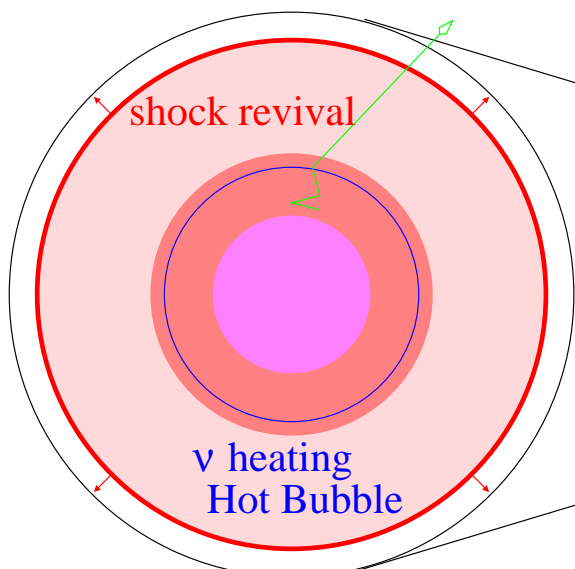
$\tau(\text{collapse}) \sim O(10-100) \text{ ms}$



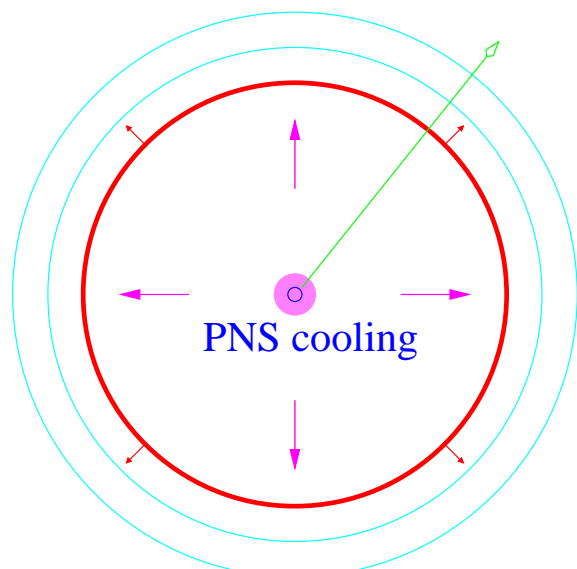
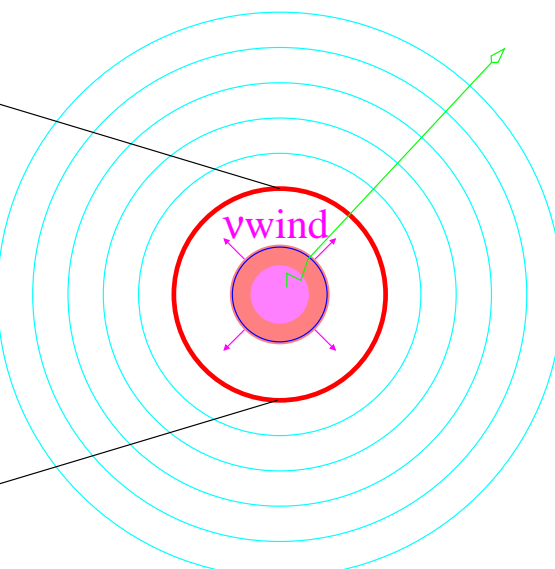
$\tau(\text{neutronization burst}) < O(10) \text{ ms}$



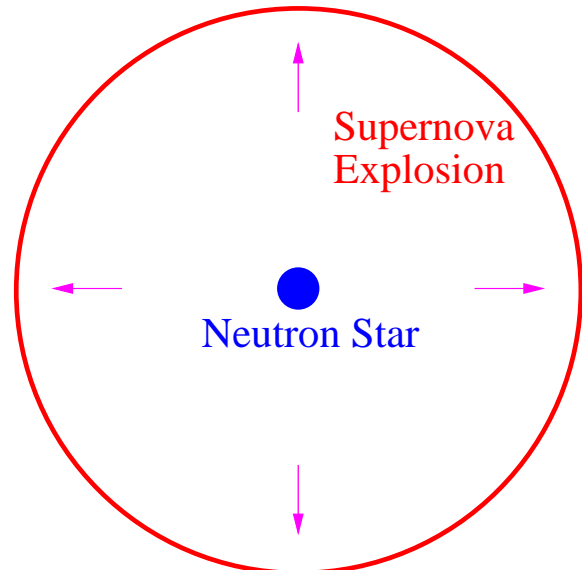
$t(\text{stall}) = O(100 \text{ ms})$



$t(\text{core exp.}) = O(1) \text{ s}$



$\tau(\text{PNS cooling}) = O(10) \text{ s}$



$$t(\text{SNE}) = \text{hours} - \text{day}$$



力二星雲

- 重力崩壊の開始

電子捕獲 (electron capture)  $e^- A \rightarrow \nu_e A'$ ,  $\lambda_\nu \gg R_{\text{core}}$

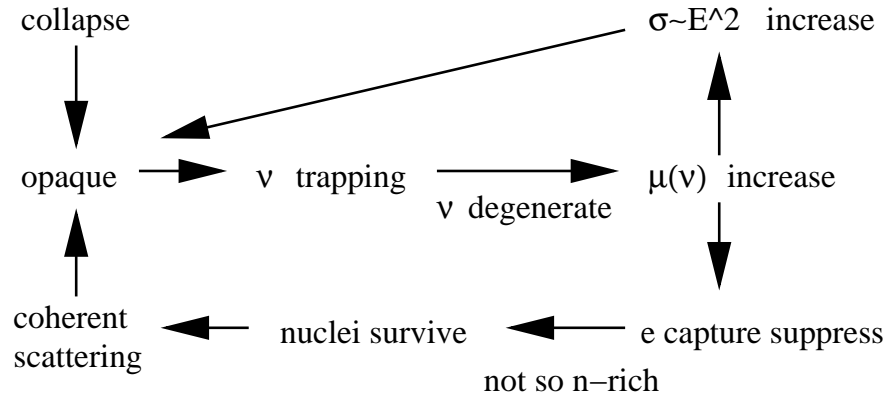
- $\nu$  trapping ( $\rho > 10^{10} - 10^{12} \text{ g/cm}^3$ )

$\nu_e$  from  $e^- A \rightarrow \nu_e A'$  and  $e^- p \rightarrow \nu_e n$

main opacity source: coherent scattering  $\nu_e A \rightarrow \nu_e A$   $\sigma \propto A^2 \omega_\nu^2$

$\rho \nearrow \rightarrow \lambda_\nu < R_{\text{core}}$ : 不透明 (neutrinosphere の出現)

$\tau_{\text{diff}} = 3R_{\text{core}}^2/c\lambda_\nu > \tau_{\text{dyn}}$  (neutrino trapping)  $\rightarrow \nu_e$  縮退



Positive feedback (Sato 1975)

SN1987A で確認

$$\left. \begin{aligned} \nu_e A &\longleftrightarrow e^- A', \quad \nu_e n \longleftrightarrow e^- p \quad (\langle \omega_{\nu_e} \rangle \lesssim \frac{5}{6} \mu_e) \\ \nu_e A &\longleftrightarrow \nu_e A, \quad \nu_e N \longleftrightarrow \nu_e N \quad (\sim \text{isoenergetic scat.}) \\ \nu_e e^- &\rightarrow \nu_e e^- \quad (\text{down scattering: } \omega_\nu \searrow, \lambda_\nu \nearrow) \end{aligned} \right) \Rightarrow Y_L \text{ trap}$$

- バウンス、衝撃波の生成

$$R_{\text{shock}} < R_{\nu \text{sphere}}$$

バウンスした内部コア  $S_c \sim O(1)$ ,  $T_c \sim O(10) \text{ MeV}$ ,  $Y_e \sim 0.3$

$\Rightarrow$  静水圧平衡状態: 原始中性子星 (PNS: protoneutron star)

$\nu_e, \bar{\nu}_e, \nu_x$ : 化学平衡 ( $\mu_{\nu_e} > 100 \text{ MeV}$ ,  $\mu_{\bar{\nu}_e} = -\mu_{\nu_e}$ ,  $\mu_{\nu_x} = 0$ )

$$M_{\text{i.c.}} \sim 1.457 M_\odot \left( \frac{Y_{L\text{trap}}}{0.5} \right)^2 = 0.6 \sim 0.9 M_\odot$$

$$E_{\text{shock}} \sim \frac{GM_{\text{i.c.}}^2}{R_{\text{i.c.}}} \propto Y_{L\text{trap}}^{10/3} \sim \text{several } 10^{51} \text{ erg}$$

$$> E_{\text{SNE}}(\text{kinetic + radiation}) \sim 10^{51} \text{ erg}$$

$$R_{\text{shock}} < R_{\nu \text{sphere}}$$

- 衝撃波が neutrinosphere を通過

衝撃波の通過した領域:  $A \rightarrow np$ ,  $e^- p \rightarrow n \nu_e$  が進行 ( $\sigma(e^- A) < \sigma(e^- p)$ )

$r(\text{shock}) < r(\nu \text{sphere})$ : 生成された  $\nu_e$  は trap されたまま

$r(\text{shock}) > r(\nu \text{sphere})$ : 生成された  $\nu_e$  は自由に出てこられる  
main opacity source だった原子核も分解される

$\Rightarrow \nu_e$  の中性子化バースト (neutronization burst)

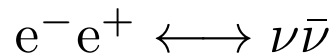
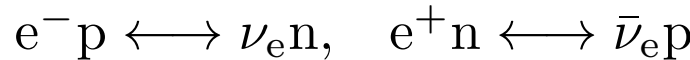
$$\tau_{\text{NB}} \sim \tau_{\text{shock propagation}} \lesssim 10 \text{ msec}, \quad L_{\nu_e \text{ NB}} \gtrsim 10^{53} \text{ erg/sec}$$

$$\Rightarrow \int L_{\nu_e \text{ NB}} dt \sim 10^{51} \text{ erg}$$

$Y_e$  分布に、deep trough を形成し、衝撃波を弱める

- 外部コア内の衝撃波の伝播

In the shocked region ( $S \sim O(10)$ , 高温低密度)



$\nu_e, \bar{\nu}_e, \nu_x$ : thermal energy を持ち出す。 $\nu_e, \bar{\nu}_e$ : 電子型レプトン数を持ちだす。

$\bar{\nu}_e, \nu_x$ : 中心へ熱を運ぶ。 $(n_{\bar{\nu}_e, \nu_x}(\text{center}) < n_{\bar{\nu}_e, \nu_x}(\text{mantle}))$

静水圧平衡の原始中性子星に、衝撃波の通過した外部コアの物質が降り積もる

降着物質の重力エネルギー → 熱エネルギー → ニュートリノ放出

$$M_{\text{PNS}} = M_{\text{i.c.}} (\sim 0.7 M_\odot) \rightarrow M_{\text{NS}} (\sim 1.4 M_\odot)$$

ニュートリノ放出による衝撃波の減衰

- 停滞した衝撃波の復活

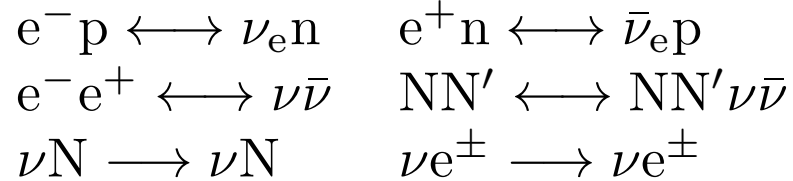
原始中性子星からのニュートリノ  $T_\nu \sim \text{数 MeV}$

shocked matter ( $r \sim \text{数 } 100 \text{ km} > R_{\nu \text{sphere}}$ )  $T \sim \text{MeV}$

$$\left. \begin{array}{l} \nu_e n \rightarrow e^- p \\ \bar{\nu}_e p \rightarrow e^+ n \\ \nu e^\pm \rightarrow \nu e^\pm \\ \nu \bar{\nu} \rightarrow e^- e^+ \end{array} \right\} \text{heating} \implies \begin{array}{l} \text{hot bubble} \\ S > 100, \rho \sim 10^5 \text{ g/cm}^3 \\ \downarrow \\ \text{delayed explosion} \quad (\tau \sim O(1) \text{ sec}) \end{array}$$

- 原始中性子星の冷却  $\tau \sim \tau_{\text{diff}} = O(10)\text{sec} \gg \tau_{\text{dyn}} \sim 1\text{msec}$ : 準静的進化  
冷却と deleptonization

hot lepton-rich PNS  $\rightarrow$  cold Neutron Star



温度が下がると、 $e^+$ がなくなるので、 $e^- e^+ \rightarrow \nu_x \bar{\nu}_x$  より、 $NN \rightarrow NN \nu_x \bar{\nu}_x$  が重要になる。

PNS = cool ( $S \sim O(1)$ ) unshocked inner core + hot ( $S \sim O(10)$ ) shocked outer mantle

PNS cooling = rapid cooling stage of the shocked outer mantle + cooling stage of the inner core

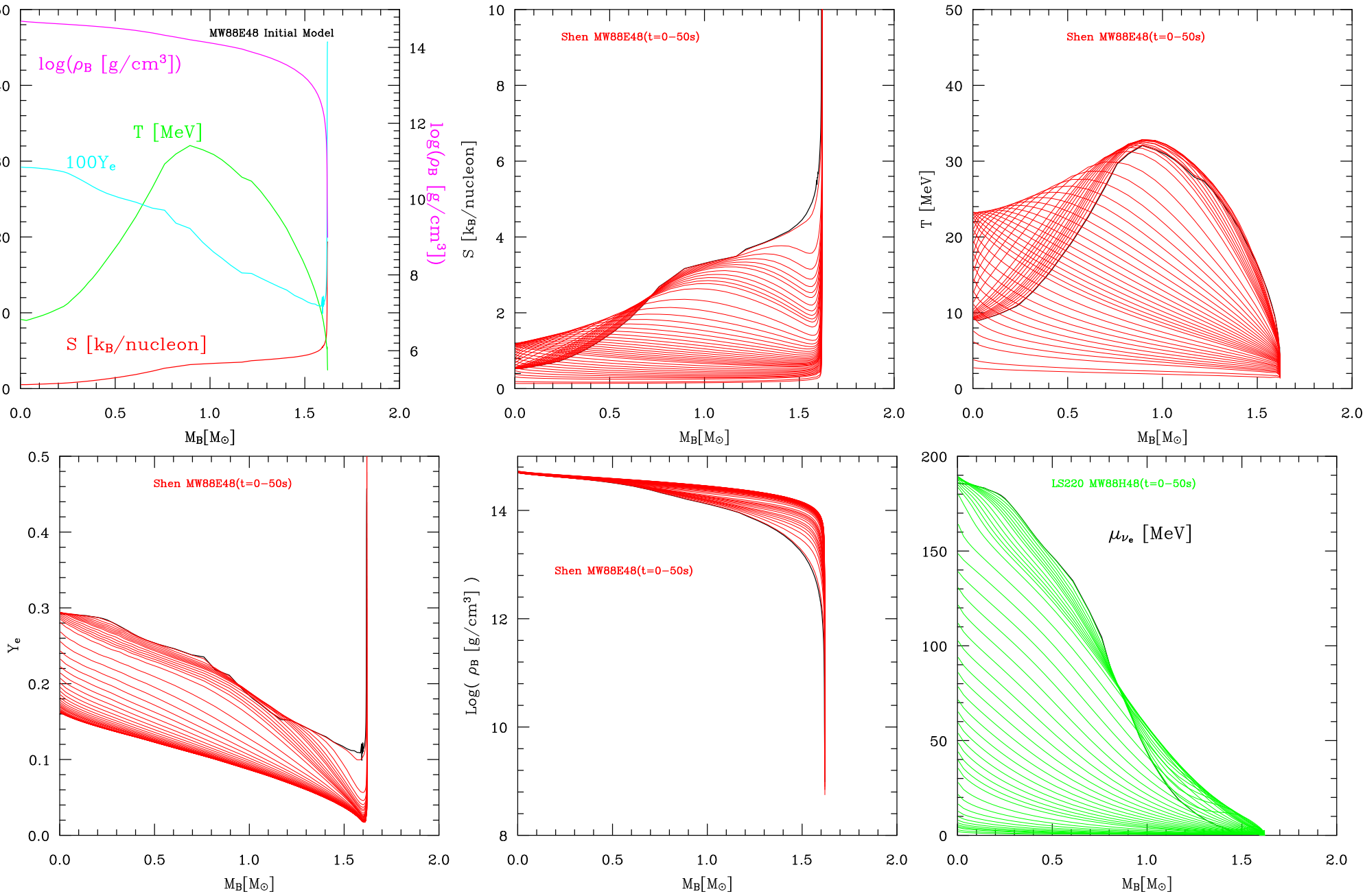
$\rho$ (mantle) is not so high  $\rightarrow$  large  $\lambda_\nu$

ニュートリノによる cooling/deleptonization

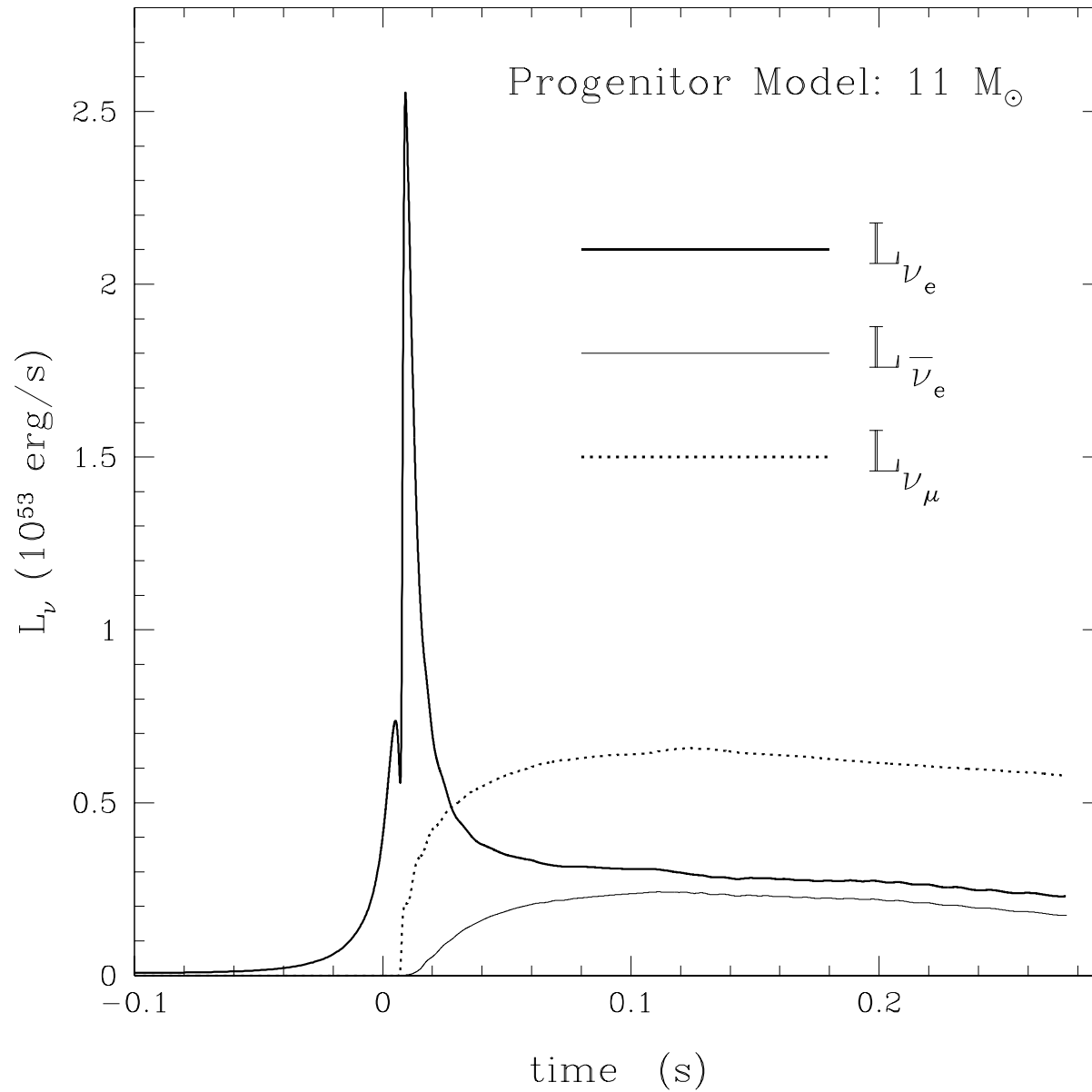
$S$ (mantle) 減少  $\rightarrow$  contraction  $\rightarrow T$ (mantle) 上昇

$T$ : mantle にピーク: 内向きの heat flux( $\bar{\nu}_e, \nu_\mu$ )  $\rightarrow S$ (core) 上昇

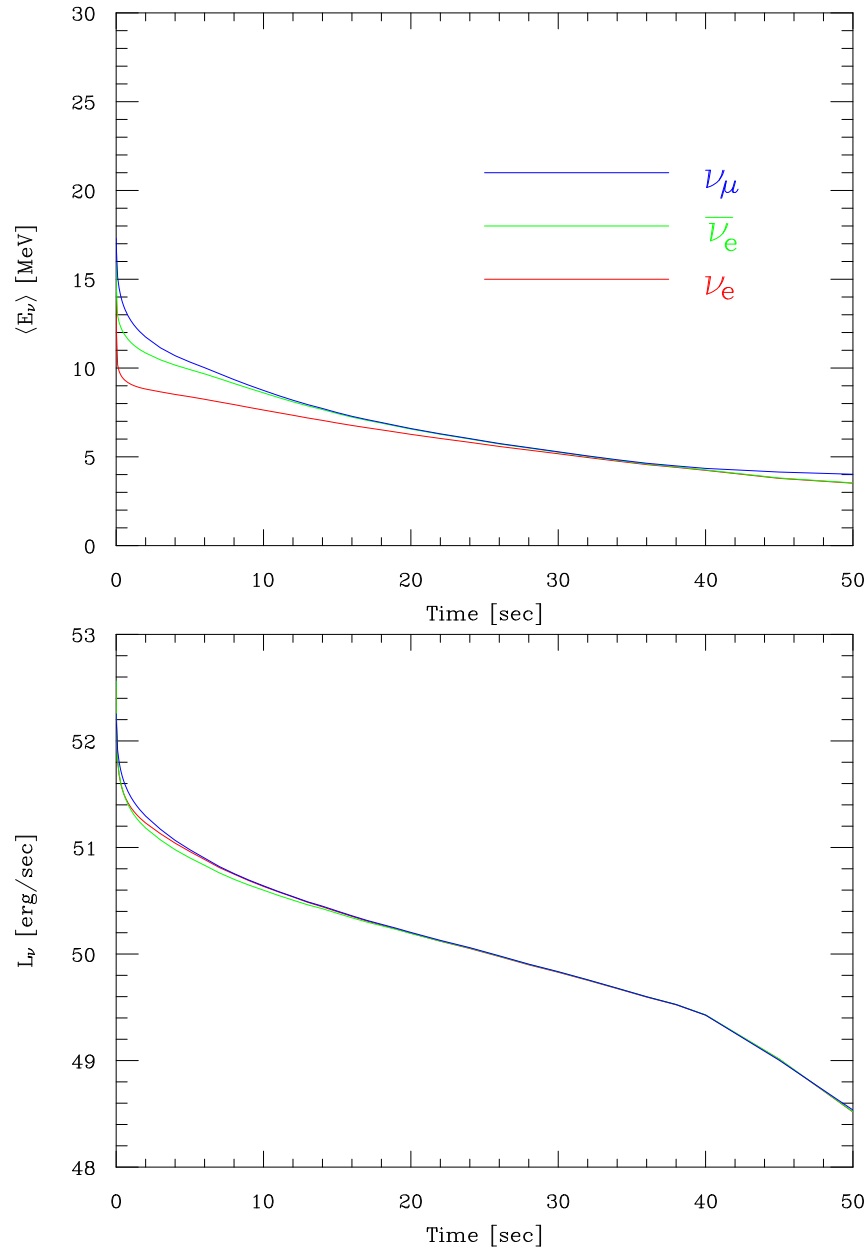
$t > 10\text{sec}$ :  $T$  分布単調減少、中心部も冷却開始



原始中性子星の冷却シミュレーション



Neutronization burst. Thompson *et al.*, ApJ 592 (2003) 434 Fig.6 (failed explosion)



cooling と deleptonization により、 $n_p$  が減少、中性子の縮退が進むため、 $\bar{\nu}_e p \rightarrow n e^+$  が抑制され、 $\sigma_{\bar{\nu}_e} \sim \sigma_{\nu_x}$ 、 $\langle \omega_{\bar{\nu}_e} \rangle \sim \langle \omega_{\nu_x} \rangle$  に向かう

原始中性子星からのニュートリノ

## ニュートリノ反応の影響

$$M_{\text{inner core}} \sim 1.457 M_{\odot} \left( \frac{Y_{L,\text{trap}}}{0.5} \right)^2 = 0.6 \sim 0.9 M_{\odot}$$

$$E_{\text{shock}} \sim \frac{GM_{\text{inner core}}^2}{R_{\text{inner core}}} \propto Y_{L,\text{trap}}^{10/3} \sim \text{several } 10^{51} \text{ erg}$$

$Y_{L,\text{trap}}$  を決めるのは、 $\nu$  trapping 前に core から出ていった  $\nu_e$  の量

$\rho < \rho_{\text{trap}}$  での電子捕獲率と Opacity が重要

higher e-cap rate, smaller opacity  $\rightarrow$  smaller  $Y_{L,\text{trap}}, E_{\text{shock}}$

$\sigma(e^- p \rightarrow \nu_e n) > \sigma(e^- A \rightarrow \nu_e A')$  なので、 $X_p \nearrow \rightarrow E_{\text{shock}} \searrow$   
 $S(\text{Fe core}) \nearrow \rightarrow X_p \nearrow \rightarrow E_{\text{shock}} \searrow$

対称エネルギー (bulk/surface) の影響は複雑?  $W_{\text{sym}} \nearrow \rightarrow X_p \searrow \rightarrow E_{\text{shock}} \nearrow$

- down scattering ( $\nu e^- \rightarrow \nu e^-, \nu A \rightarrow \nu A^*$ ) により、 $\omega_{\nu} \searrow, S \nearrow \rightarrow \lambda_{\nu} \nearrow$   
 $Y_{L,\text{trap}} \searrow, E_{\text{shock}} \searrow$

### ● 電子捕獲率

Bruenn'85:  $p(f_{7/2}) \rightarrow n(f_{5/2})$  の Gamow-Teller transition

$N < 40$ : possible,  $N \geq 40$ : impossible

shell model に基づく新しい電子捕獲率/ $\beta$ 崩壊率の計算 (LMP: Langanke and Martinez-Pinedo): これまで一般的だった Brueen 方式 ( $N > 40$  での電子捕獲反応抑制) や FFN(Fuller, Fowler and Newman) と異なる結果

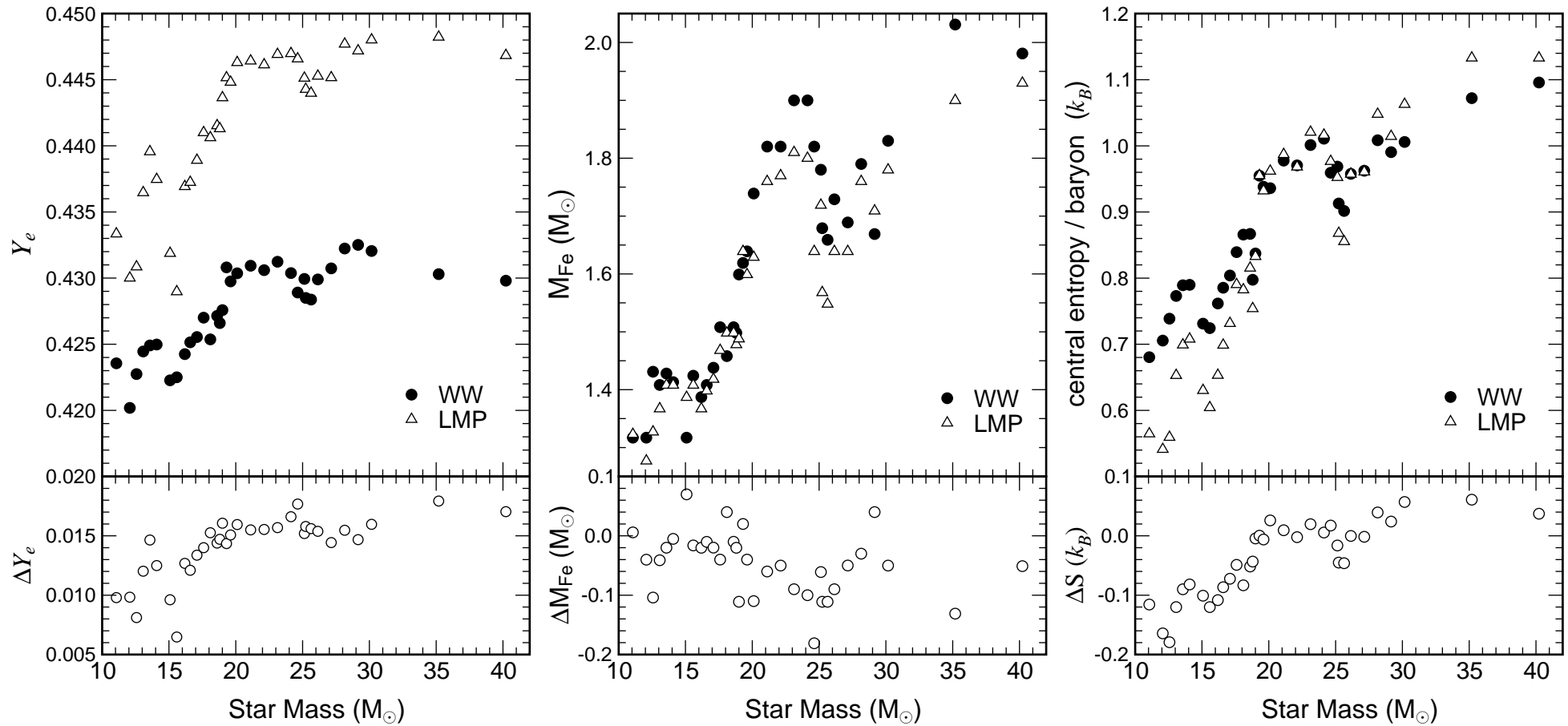


Figure 1: weak int. rate と Fe コア: WW(FFN) と LMP の比較。G. Martinez-Pinedo *et al.*, astro-ph/0412091

LMP ( $A = 45 - 65$ , Shell model、許容遷移のみ): GT strength  $\searrow$  電子捕獲率  $\searrow$   $Y_e \nearrow$   $M_{\text{Fe core}} \searrow$

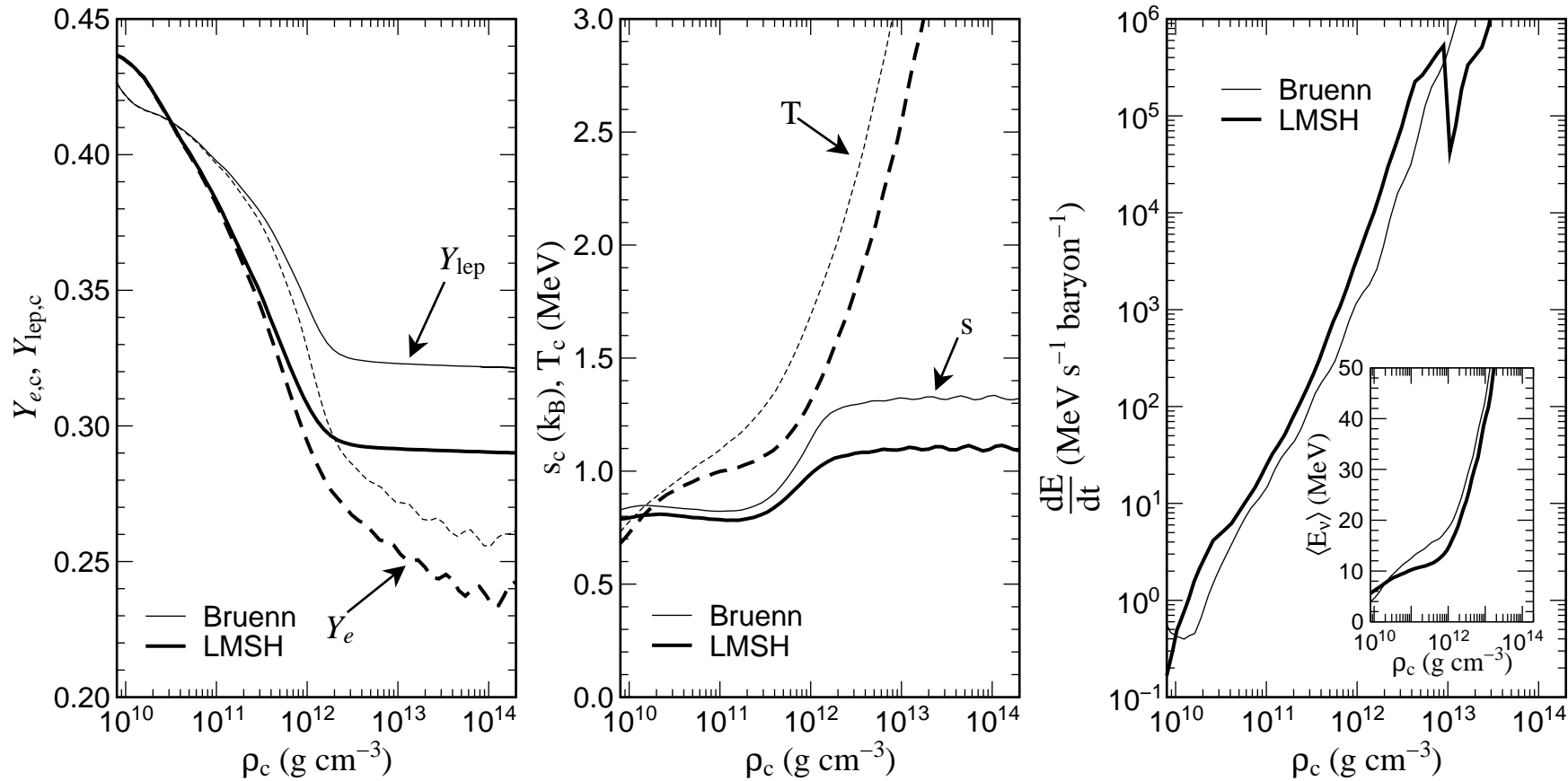


Figure 2: 電子捕獲反応率と  $15M_{\odot}$  星のコアの重力崩壊。G. Martinez-Pinedo *et al.*, astro-ph/0412091

LMS:  $N > 40$  の原子核による電子捕獲率を評価 ( $A = 66 - 112$  Shell Model Monte Carlo + RPA)

LMSH: FFN( $A < 45$ ) + LMP( $A = 45 - 65$ 、許容遷移のみ) + LMS( $A = 66 - 112$ ), NSE

$X_p$  だけが重要ではない、電子捕獲率  $\nearrow Y_{L\text{trap}} \searrow$

多核種が混在する NSE での、電子捕獲率の評価が重要

Juodagalvis, Langanke *et al.*, 2010, FFN/Shell model/Shell Model Monte Carlo+RPA に加え  
 Fermi-Dirac parameterization+RPA( $Z = 28 - 70, N = 40 - 160$ ), electron screening

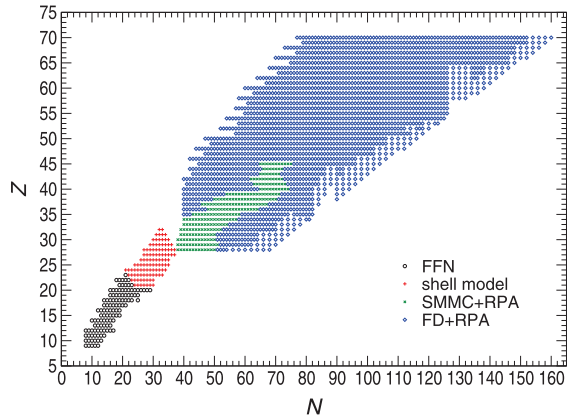


Fig. 1. (Color online.) Nuclei included in the calculation of the NSE-averaged rates and spectra. The  $sd$  pool is marked by circles, the shell model pool is marked by pluses, the SMMC + RPA pool is marked by crosses, and the FD + RPA pool is marked by diamonds.

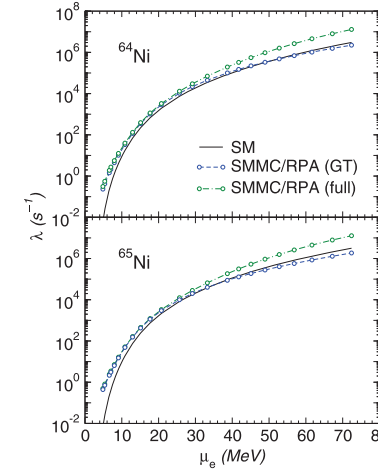


Fig. 2. (Color online.) A comparison of the electron capture rates on  $^{64,65}\text{Ni}$  calculated from the diagonalization shell model (only allowed contributions) and the hybrid SMMC + RPA model (both allowed and forbidden contributions). Stellar conditions of the  $25M_{\odot}$  trajectory (see Table 1) are used.

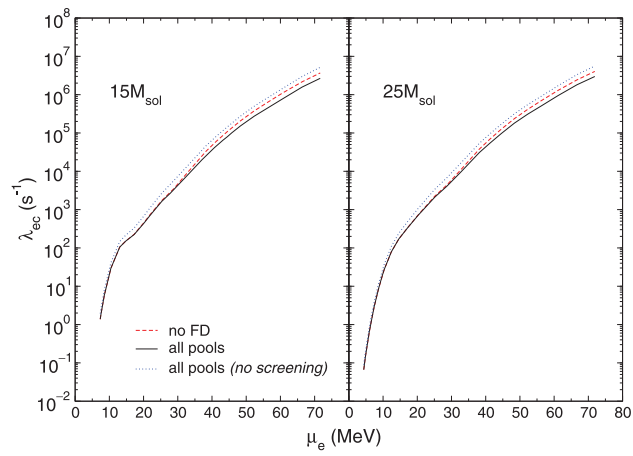


Fig. 10. (Color online.) Pool-averaged electron capture rates calculated along the stellar trajectories for the  $15M_{\odot}$  and  $25M_{\odot}$  progenitor stars. The rates based on the sum of all pools of nuclei are shown by solid lines. The dashed lines show the average rate when the FD + RPA pool is omitted. The dotted lines show the average rate for the sum of all pools when the screening effects to the rates are neglected.

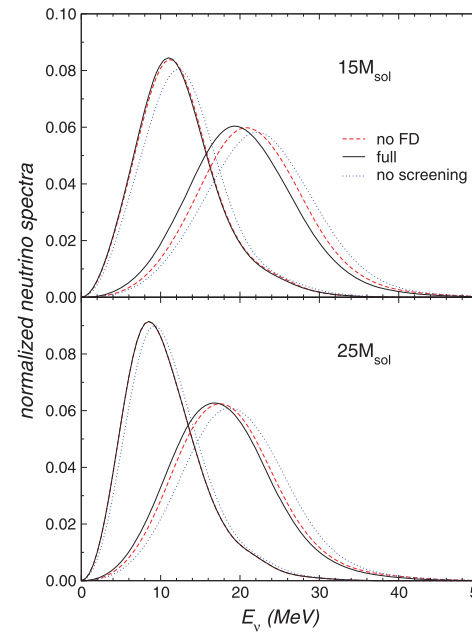


Fig. 11. (Color online.) Pool-averaged emitted neutrino spectra for the  $15M_{\odot}$  and  $25M_{\odot}$  trajectories. The line legend is the same as in Fig. 10. Two stellar conditions are used in each case corresponding to snapshot numbers 10 and 15 of the respective trajectory. For snapshot number 10 in the lower panel the curves “no FD” and “full” coincide.

electron screening は、電子捕獲率を下げる

$\rho \sim 10^{11}, 10^{12} \text{ g/cm}^3$

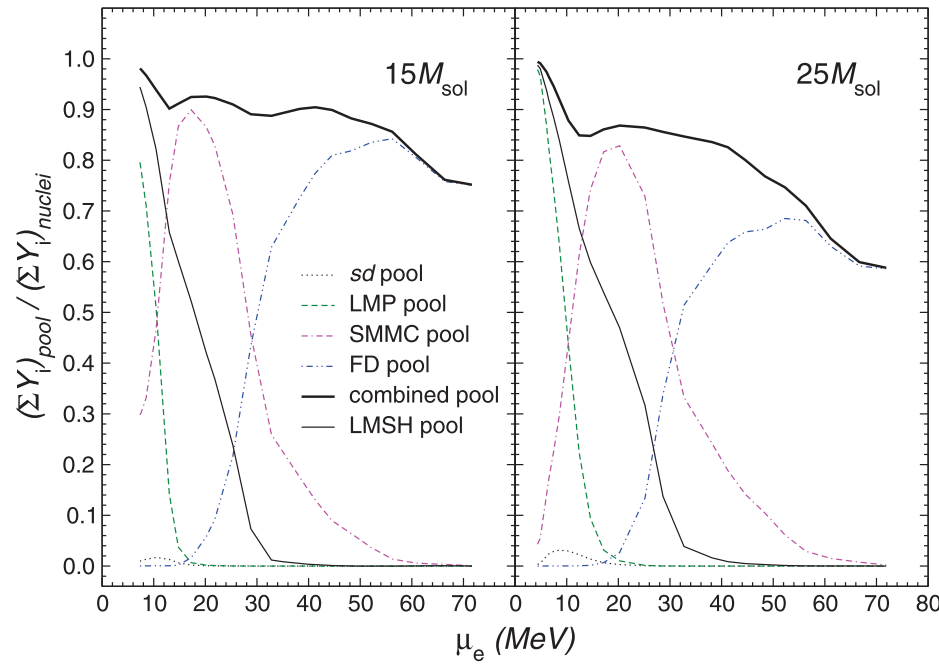


Fig. 6. (Color online.) Fraction of nuclei covered by the various pools of nuclei as defined in the text. The fractions have been calculated for the two stellar trajectories given in Table 1. The pools are *sd* (dotted line), *LMP* (dashed line), *SMMC + RPA* (double-dash-dotted line), and *FD + RPA* (dash-double-dotted line). Solid lines show the summed pool coverage. Thick solid lines show present pool coverage, and thin solid lines show coverage by the *LMSH* pool.  $(\sum_i Y_i)_{\text{nuclei}}$  is calculated by summing over all nuclei except protons, neutrons and  $\alpha$  particles.

# NSE EOS (Furusawa *et al.*, ApJ738, 2011): 電子捕獲率だけでなく散乱率にも影響

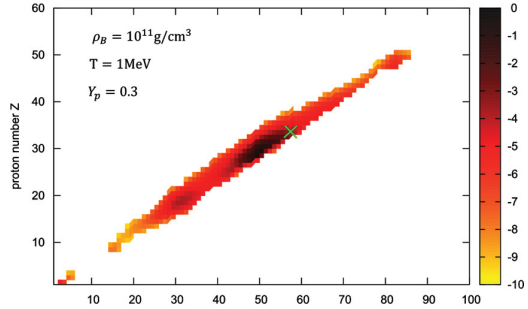


Figure 1. Mass fractions in  $\log_{10}$  of nuclei in the  $(N, Z)$  plane for  $\rho_B = 10^{11} \text{ g cm}^{-3}$ ,  $T = 1 \text{ MeV}$ , and  $Y_p = 0.3$ . The cross indicates the representative nucleus for the H. Shen EOS under the same condition.

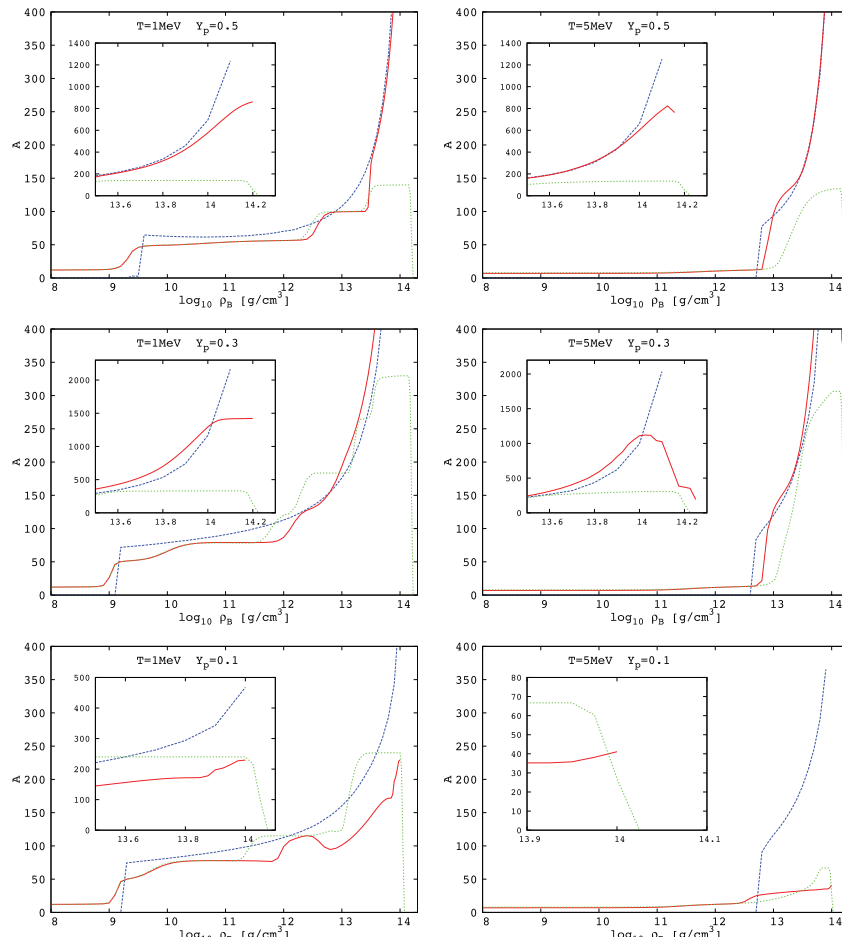


Figure 5. Average mass number,  $\bar{A}$ , of heavy nuclei with  $Z \geq 6$  for our EOS (solid red lines) and Hempel's EOS (dotted green lines) together with the mass number of representative nucleus for H. Shen's EOS (dashed blue lines) as a function of density for  $T = 1 \text{ MeV}$  and  $Y_p = 0.1, 0.3, 0.5$ . The insets are the close-ups of the high density regimes.

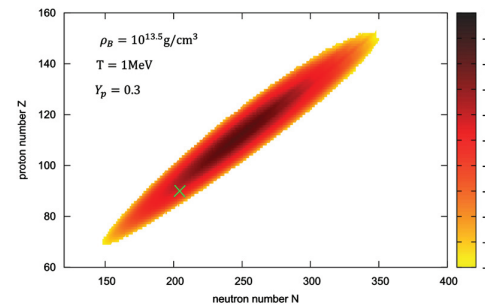


Figure 2. Mass fractions in  $\log_{10}$  of nuclei in the  $(N, Z)$  plane for  $\rho_B = 10^{13.5} \text{ g cm}^{-3}$ ,  $T = 1 \text{ MeV}$ , and  $Y_p = 0.3$ . The cross indicates the representative nucleus for the H. Shen EOS under the same condition.

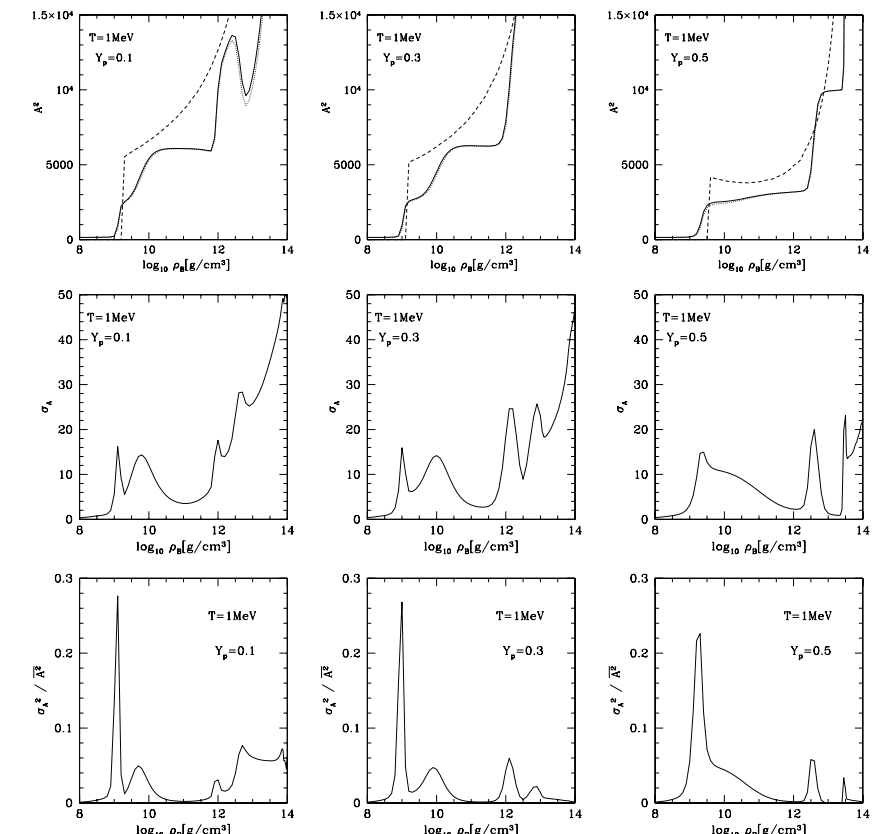


Figure 6. Square of mass numbers (top), the standard deviation of mass number,  $\sigma_A$  ( $= \sqrt{\bar{A}^2 - \bar{A}^2}$ ) (middle), and the dispersion normalized by the average mass number squared,  $\sigma_A^2 / \bar{A}^2$  (bottom), of heavy nuclei with  $Z \geq 6$  for  $T = 1 \text{ MeV}$  and  $Y_p = 0.1$  (left), 0.3 (middle), and 0.5 (right). In the top panels, the solid and dotted lines show the average mass number squared,  $\bar{A}^2$ , and the square of average mass number,  $\bar{A}^2$ , in our EOS, whereas the dashed lines display the mass number squared of the representative nucleus for the H. Shen EOS.

$A$  の分散は大きくないが、single nucleus EOS とは  $A^2$  平均が大きく異なる

- ion screening (Horowitz 1997, Bruenn and Mezzacappa 1997)  
 Coulomb effect → ions in correlated states  
 $\sigma(\nu A \rightarrow \nu A)$  decreases when the wave length of neutrinos > ion separation

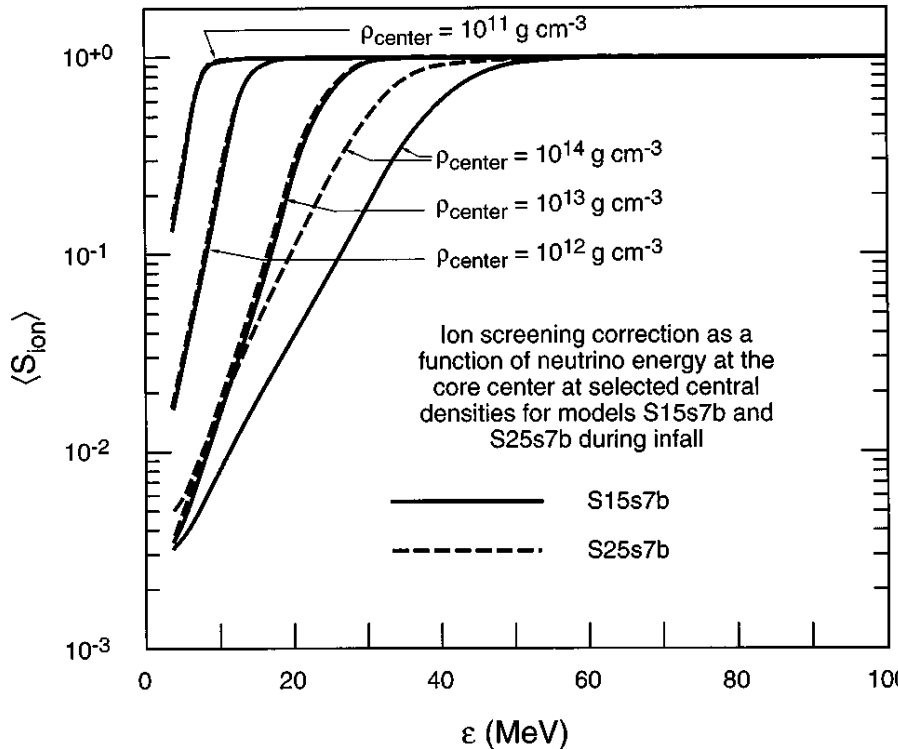


FIG. 2. The angle-averaged ion screening correction  $\langle S_{\text{ion}}(\epsilon) \rangle$  at the core center for selected central densities, as a function of neutrino energy, for models S15s7b and S25s7b.

コアの重力崩壊のシミュレーション (Bruenn and Mezzacappa 1997)

$$\Delta Y_{L\text{trap}} = -0.015 \text{ not so drastic}$$

(narrow  $\omega_\nu$  window is affected)

$$Y_{L\text{trap}} \searrow \Rightarrow M_{\text{inner core}} \searrow (2 - 6\%) \Rightarrow E_{\text{shock}} \searrow$$

- 核子制動輻射  $NN' \longleftrightarrow NN'\nu\bar{\nu}$

Suzuki and Ishizuka: One Pion Exchange model

$\nu_x\bar{\nu}_x$ 生成:  $\rho > 10^{13} \text{g/cm}^3, T \sim 10 \text{MeV}$  で低エネルギー $\nu$ に対して  $e^-e^+ \rightarrow \nu_x\bar{\nu}_x$  を上回る。

低エネルギーニュートリノを enhance  $L_{\nu_x} \nearrow, \langle \omega_{\nu_x} \rangle \searrow$

一方 multiple scattering suppression (Raffelt and Seckel 1991) は低エネルギーニュートリノの核子制動輻射を抑制

(Hannestad and Raffelt, Raffelt and Seckel 1998, Shen and Suzuki, Burrows *et al.* 2000)

- $\nu N$  散乱によるエネルギー交換:  $\rho > 10^{11} \text{g/cm}^3, \omega_\nu > 10 \text{MeV}$  で ES を上回り  $\langle \omega_{\nu_x} \rangle \searrow$
- $\nu NN$  散乱によるエネルギー交換:  $\nu N$  散乱の影響に埋もれる
- $\nu N \leftrightarrow eN'$  に対する weak magnetism ( $\leftarrow$  核子の異常磁気モーメント):  $\sigma_{\bar{\nu}_e p}(20 \text{MeV}) : -15\%$

- effective mass, nucleon density/spin fluctuations  
 $\Rightarrow$  reduction of opacity  $\rightarrow L_\nu \nearrow$   
(Sawyer 1995, München group 1995-1998, Burrows and Sawyer 1998-1999,  
Reddy *et al.* 1998-1999, Yamada and Toki 1999-2000)  
 $\nu N$  反応に対する多体効果(密度・スピン相関):  $\rho > 10^{14} \text{ g/cm}^3$  で  $\sigma \rightarrow \frac{1}{2} \sim \frac{1}{3}$ 、  
 $L_\nu(t > 100\text{ms}) \nearrow$

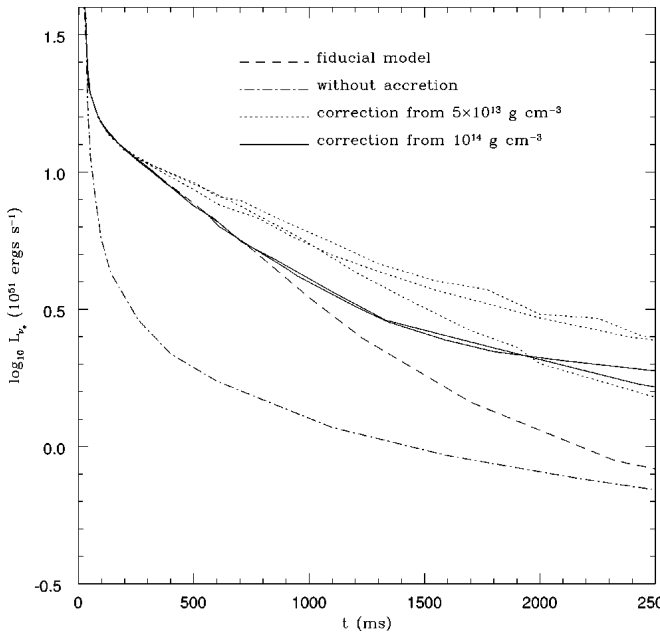


FIG. 11.  $\log_{10}$  of the electron neutrino luminosity ( $L_{\nu_e}$ ) in  $10^{51} \text{ ergs s}^{-1}$  versus time after bounce in ms, with and without accretion. For the accretion models, total opacity suppression factors of 0.3, 0.1, and 0.05 were assumed above  $5 \times 10^{13} \text{ g cm}^{-3}$  and of 0.3 and 0.1 were assumed above  $10^{14} \text{ g cm}^{-3}$ . The fiducial model is dashed, the model without accretion is dot-dashed, the models with correction above  $5 \times 10^{13} \text{ g cm}^{-3}$  are dotted, and those with correction above  $10^{14} \text{ g cm}^{-3}$  are solid. On this plot, the models with the largest corrections have the highest luminosities after 2500 ms. The comparisons between the dashed curve and all others are the most germane.

- 軽元素との反応  
 $^2\text{H}, ^3\text{H}, ^3\text{He}, ^4\text{He}$

Sumiyoshi and Röpke

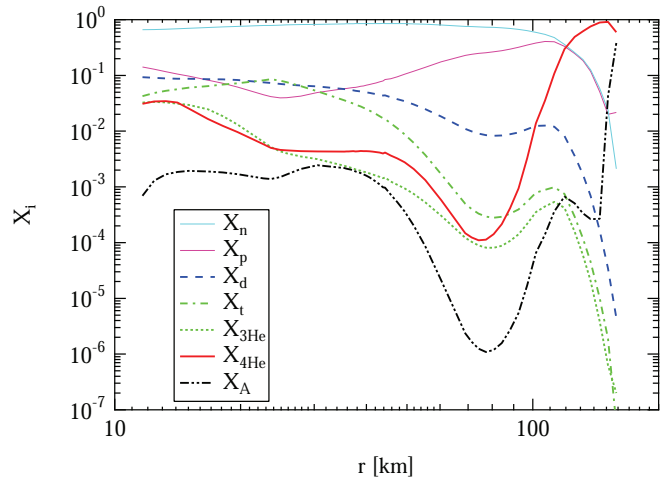
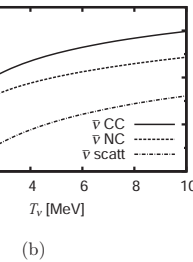
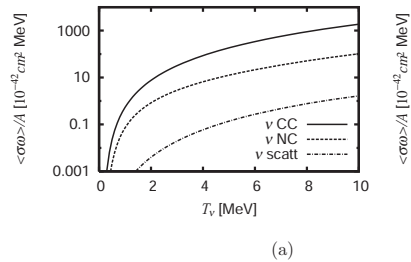


FIG. 2: (Color online) Mass fraction  $X_i$  of light clusters as function of the radius for the post-bounce supernova core shown in Fig. 1.

Sumiyoshi and Röpke PRC77 (2008) 055804



(a)

(b)

FIG. 3: Thermal average of energy transfer cross sections. The solid and dotted curves in (a) ((b)) show the cross sections for  $\nu_e d \rightarrow e^- pp(\nu\text{CC})$  and  $\nu d \rightarrow \nu pm(\nu\text{NC})$  ( $\bar{\nu}_{ed} \rightarrow e^+ nn(\bar{\nu}\text{CC})$  and  $\bar{\nu}d \rightarrow \bar{\nu}pm(\bar{\nu}\text{NC})$ ), respectively. The dot-dashed curve in (a) and (b) shows cross section for the elastic  $\nu d$  scattering.

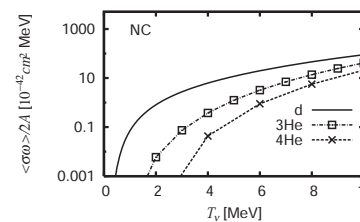
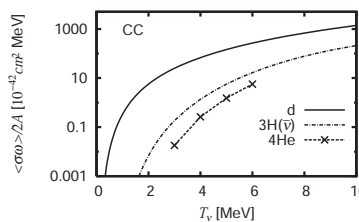


FIG. 4: Averaged energy transfer cross sections in unit of  $10^{-42} \text{ MeV cm}^2$ . The solid, dashed and dash-dotted curves show the  $\nu d$ ,  $\nu^4\text{He}$  and  $\nu^3\text{H}$  (left panel) and  $\nu^3\text{He}$  (right panel) cross sections, respectively. (See the main text for the references on  $A=3, 4$  nuclei cross sections.)

Nakamura *et al.*, 2009, d の分解がレ 加熱に効くかも

## ✓ 反応率は状態方程式と密接に関連: EOS とセットでテーブル化が必要

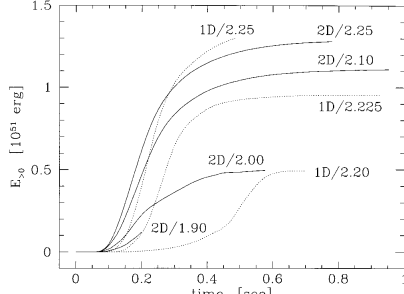
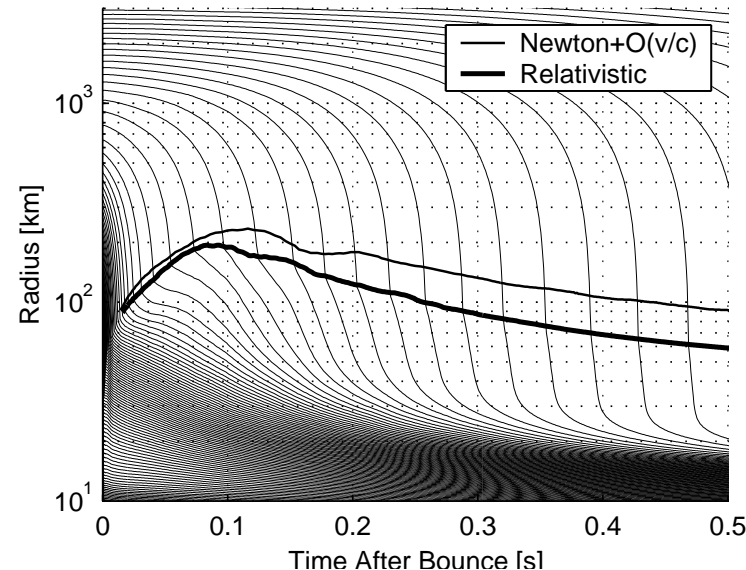
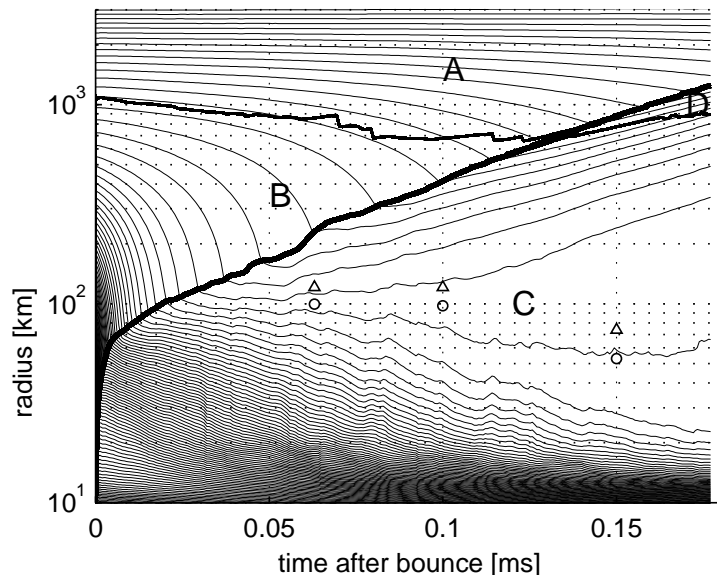


FIG. 1.—Explosion energies vs. time after the start of the simulations ( $\sim 25$  ms after bounce) for exploding one-dimensional (dotted lines) and two-dimensional models (solid lines). The numbers denote the initial  $\nu_e$  and  $\bar{\nu}_e$  luminosities in  $10^{52}$  ergs  $s^{-1}$ .

ニュートリノ加熱率の正確な評価が重要  $1D/2.10$ : no exp.  $\Leftrightarrow 1D/2.20$ : exp. (Janka and Müller, ApJ 448 (1995) L109, Fig.1)



**mistake:**  $\sigma(\nu N \rightarrow \nu N)$  too small  $\Rightarrow$  **Explosion!**  
Liebendörfer *et al.*, astro-ph/0006418 v1 Fig.4

No Explosion!. NH  $13M_\odot$ , GR Boltzmann, LS EOS+Si burning,  $S = 103$ ,  $E = 12$ ,  $A = 6, 3\nu$   
GR  $\rightarrow$  compact PNS  $\rightarrow T \nearrow L_\nu \nearrow$ ,  
**Boltzmann  $\rightarrow$  heating rate  $\nearrow$**   
Liebendörfer *et al.*, Phys.Rev. D63 (2001) 103004 (astro-ph/0006418 v2) Fig.6